Microplastics in the Northwestern Pacific: Abundance, distribution, and characteristics

Science of the Total Environment 650 (2019) 1913–1922

Contents lists available at ScienceDirect

Science of the Total Environment

journal homepage: www.elsevier.com/locate/scitotenv

Microplastics in the Northwestern Pacific: Abundance, distribution, and characteristics

Zhong Pan [a], Huige Guo [a], Hongzhe Chen [a], Sumin Wang [a], Xiuwu Sun [a], Qingping Zou [b], Yuanbiao Zhang [a,*], Hui Lin [a,*], Shangzhan Cai [c], Jiang Huang [c]

[a] Laboratory of Marine Chemistry and Environmental Monitoring Technology, Third Institute of Oceanography, State Oceanic Administration, Xiamen 361005, China
[b] The Lyell Centre for Earth and Marine Science and Technology, Institute for Infrastructure and Environment, Heriot-Watt University, Edinburgh, UK
[c] Ocean Dynamics Laboratory, Third Institute of Oceanography, State Oceanic Administration, Xiamen 361005, China

HIGHLIGHTS

- The microplastics were surveyed and the physical oceanographic parameters in the Northwestern Pacific were measured.
- Microplastics are prevalent with various colors, sizes, shapes and chemical compositions in the open sea.
- The mechanisms for microplastic distribution were proposed by chemical composition and the physical oceanographic data.

GRAPHICAL ABSTRACT

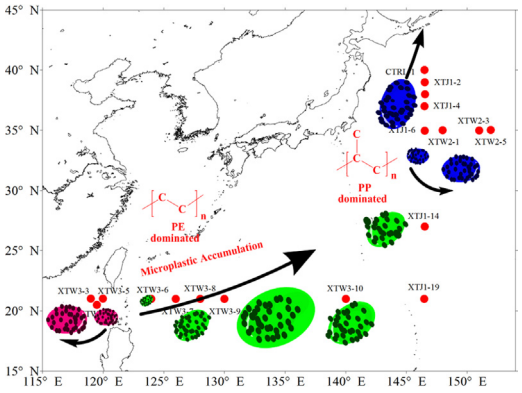

ARTICLE INFO

Article history:
Received 21 March 2018
Received in revised form 18 September 2018
Accepted 18 September 2018
Available online 19 September 2018

Editor: Kevin V. Thomas

Keywords:
Microplastic
Northwestern Pacific
Abundance
Chemical fingerprint
Distribution

ABSTRACT

Prevalence of microplastics (MPs) throughout the world's oceans has raised growing concerns due to its detrimental effects on the environment and living organisms. Most recent studies of MPs, however, have focused on the estuaries and coastal regions. There is a lack of study of MPs pollution in the open ocean. In the present study, we conducted field observations to investigate the abundance, spatial distribution, and characteristics (composite, size, color, shape and surface morphology) of MPs at the surface of the Northwestern Pacific Ocean. Samples of MPs were collected at 18 field stations in the Northwestern Pacific Ocean using a surface manta trawl with a mesh size of ~330 μm and width of 1 m from August 25 to September 26, 2017. The MPs were characterized using light microscopy, Micro-Raman spectroscopy, and scanning electron microscopy (SEM). Our field survey results indicate the ubiquity of MPs at all stations with an abundance from 6.4×10^2 items km^{-2} to 4.2×10^4 items km^{-2} and an average abundance of 1.0×10^4 items km^{-2}. The Micro-Raman spectroscopic analysis of the MPs samples collected during our field survey indicates that the dominant MPs is polyethylene (57.8%), followed by polypropylene (36.0%) and nylon (3.4%). The individual chemical compositions of MPs from the stations within the latitude range 123–146°E are comparable with each other, with PE being the dominating composition. Similar chemical fingerprints were observed at these field stations, suggesting that the MPs originated from similar sources. In contrast, the major MPs at the field stations adjacent to Japan is polypropylene, which may originate from the nearby land along the coast of Japan. Physical oceanography

* Corresponding authors.
E-mail addresses: zhangyuanbiao@tio.org.cn (Y. Zhang), linhui@tio.org.cn (H. Lin).

https://doi.org/10.1016/j.scitotenv.2018.09.244

parameters were also collected at these stations. The spatial distribution of MPs is largely attributed to the combined effects of flow pattern, adjacent ocean circulation eddies, the Kuroshio and Kuroshio Extension system.

1. Introduction

The world has seen explosive growth in the production and consumption of plastic materials in the past decades due to their versatility, lightweight, low cost, durability, and pliability. The annual plastic production surged 20% in five years from 279 million tons in 2011 to 335 million tons in 2016 (PlasticsEurope, 2018; Zhang, 2017). The sheer volume of plastic pollution in the environment owes largely to the persistence of plastics. A substantial amount of plastics end up in waterways, particularly in the marine environment. It was estimated that 4.8–12.7 million tons of plastic wastes were pumped into the ocean in 2010. This number is expected to grow by an order of magnitude by 2025 (Jambeck et al., 2015; Kooi et al., 2017). MPs were initially defined as the microscopic plastic debris in the 20 μm scale (Thompson et al., 2004) and later as the plastic particles <5 mm in diameter (Andrady and Neal, 2009; NOAA, 2016), albeit not a standard definition. MPs can be either primary or secondary MPs (Li et al., 2018; Piñon-Colin et al., 2018). Primary MPs comes from personal care products in the form of microbeads (e.g., exfoliating facial cleansers, cosmetics.), plastic products (e.g., resin pellet.), and synthetic textiles. A portion of MPs comes from fiber-containing laundry effluents released into the environment since wastewater treatment plants fail to retain and eliminate MPs. For example, Browne et al. reported that ~1900 synthetic fibers may be shed from one synthetic garment during each washing cycle (Browne et al., 2011; Cauwenberghe et al., 2015). A large marine plastic debris becomes brittle with time and breaks into small pieces, so-called secondary MPs through various environmental processes such as biological activities, UV irradiations, mechanical abrasions, temperature fluctuations, wind and wave actions (Auta et al., 2017; Barnes et al., 2009; Bergmann et al., 2017; Ling et al., 2017).

The abundant and widely spread floating marine plastics around the globe introduce massive amounts of MPs into the marine environment, which constitute the vast majority of buoyant marine plastics (Mauro et al., 2017). MPs have been identified across the worldwide's oceans, from nearshore to offshore and pelagic regions, at sea surfaces, in water columns and seabed sediments, and from the Arctic to the Antarctic (Abayomi et al., 2017; Cauwenberghe et al., 2013; Isobe et al., 2017; La Daana et al., 2017; Lots et al., 2017; Lusher et al., 2015; Waller et al., 2017; Zhang et al., 2017). As the infinitesimal fragments of plastic, MPs are expected to increase exponentially with shrinking size and time due to its longevity (Cózar et al., 2014; Kooi et al., 2017). As a result, the MP abundance is likely to grow dramatically in the future unless effective mitigation measures are implemented in a timely fashion.

Persistent organic pollutants (POPs), including polychlorinated biphenyls (PCBs), polycyclic aromatic hydrocarbons (PAHs), and polybrominated diphenyl ethers (PBDEs), have a great propensity to cling to MPs, due to their hydrophobic nature (Mato et al., 2001; Ogata et al., 2009). MPs may also adsorb heavy metals such as lead, copper and nickel (Brennecke et al., 2016; Rochman et al., 2014). It follows that MPs act as vehicles for transferring toxic chemicals through trophic levels (Bakir et al., 2012; Browne et al., 2008; Teuten et al., 2007; Wessel et al., 2016). MPs may be ingested by marine organisms and cause blockage of metabolic channels (e.g., alimentary tract and gut), physical damages, reduced appetite, altered feeding behavior and fatigue. MPs may transfer their associated organic contaminants or toxic additives to living organisms and hinder the growth, development, and reproduction of marine life (Cole et al., 2015; Hamlin et al., 2015; Von Moos et al., 2012; Watts et al., 2015; Wegner et al., 2012; Wright et al., 2013a). Environmental impacts of MPs have raised growing public concerns. Furthermore, there is an increasing awareness of a growing threat from MPs to human health due to human exposures to MPs and their associated toxins via food chains or inhalation of MPs in the air (Vethaak and Leslie, 2016; Wright and Kelly, 2017).

The growing concerns of adverse impacts of MPs have spurred a wide array of studies of the abundance, distribution, fate, and transport of MPs in the marine environment. Majority existing studies have focused on the widespread occurrence and distribution of MPs in the aquatic environment, however, research on abundance, distribution, and characteristics of MPs in the pelagic zone is currently lacking. The objective of the present study is to conduct field observations to investigate the abundance, distribution, and characteristics (composite, size, color, shape and surface morphology) of MPs in the Northwestern Pacific Ocean. MPs are characterized using light microscopy, Micro-Raman spectroscopy, and scanning electron microscopy (SEM). Physical oceanography parameters were also collected at these stations. The sources, distributions, and generation mechanisms of MPs in the pelagic zone are evaluated based on the field observations at these 18 stations across the Northwestern Pacific Ocean and link with flow patterns, adjacent ocean circulation eddies, the Kuroshio Current and Kuroshio Extension system.

2. Materials and methods

Although the benchmark methodology for MPs analysis has not been established, the following procedure has been used widely: (1) MPs collection; (2) MPs isolation (separation, digestion, filtration, drying); (3) visual identification; (4) Characterization by Fourier Transform Infrared Spectroscopy (FTIR)/Micro-Raman/Scanning Electron Microscopy-Energy Dispersive Spectroscopy (SEM-EDS); (5) identity assignment (Ribeiro-Claro et al., 2016). In the present study, a revised National Oceanic and Atmospheric Administration (NOAA) protocol (NOAA, 2015) is adopted for MPs sample collections and preparations.

2.1. Study area

Surface MPs sampling were collected at 18 stations across the Northwestern Pacific Ocean (cf. Fig. 1 and Table 1). Three stations XTW3-3, XTW3-4, and XTW3-5 are located evenly along the same latitude in the west of Luzon Strait (118–120°E). Six stations (XTW3-6, XTW3-7, XTW3-8, XTW3-9, XTW3-10, and XTJ3-19) are located in the latitude direction from 123 to 146°E. Another six stations (XTJ3-19, XTJ1-14, XTJ1-6, XTJ1-4, XTJ1-3, and XTJ1-2) are located in the longitudinal direction from 20 to 38°N. Four stations XTJ1-6, XTW2-1, XTW2-3, and XTW2-5 span eastward from 146 to 151°E. Locations of MPs field stations, sampling dates, abundance, and chemical composition of MPs are listed in Table 1 and illustrated in Fig. 1.

2.2. MPs sampling

A large volume of water samples are required during the MPs field survey, due to low concentration of MPs in the ocean (Bergmann et al., 2015), particularly in the pelagic zone. Floating MPs were collected from 18 stations (Fig. 1) in the Northwestern Pacific using a surface manta trawl with a mesh size of ~330 μm and width of 1 m from August 25 to September 26, 2017. The manta trawl was deployed to sea surface via a reel-operated lift on the side of the research vessel. The angle between trawling and shipping route is about 20°. The MPs at the ocean surface were sampled by trawling horizontally between

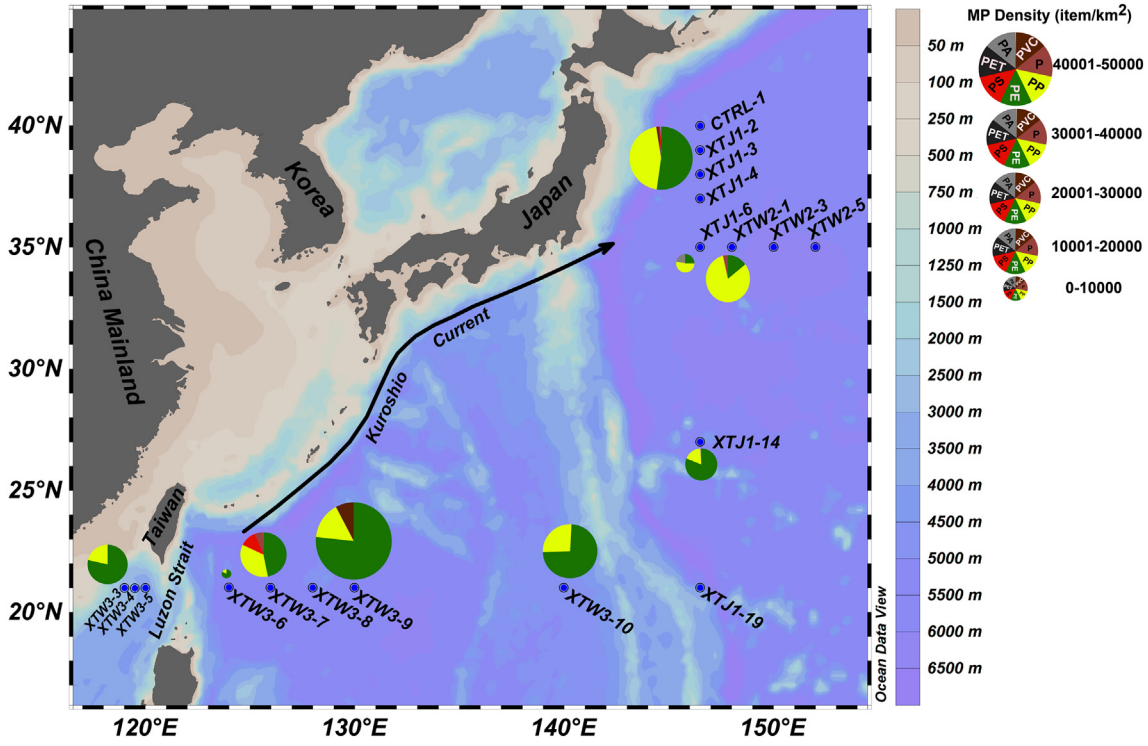

Fig. 1. Sampling sites and MPs characterization in the Northwestern Pacific. Blue dots represent the sampling locations. Size of pie charts reflects the MPs concentration. Colors of pie charts indicate the compositions of MPs, Green: PE; Yellow: PP; Red: PS; Dark Burgundy: PVC; black: PET; Gray: PA; Light Burgandy: P.

50 and 240 min at a speed of 1.0 to 3.0 knots at each field station. The trawling distance is estimated using the GPS data recorded at the beginning and end of trawling. The sampling area is estimated as the product of trawling length and net width. When the net is clogged by debris such as phytoplankton, the sampling is suspended and restarted using a clean manta net. At the end of the trawling, the net was lifted at a speed of 0.5 m s^{-1} and rinsed with natural seawater onsite to drive all the samples inside the net down to the bottom of the sampling bottle and wash away the impurities outside the net. The used net was collected for further processing in the laboratory. Plastic and other debris >5 mm in diameter were picked up by steel tweezers and put into glass bottles. The sample in the collector attached to the bottom of the net was then transferred to a 500-mL glass vial. Meanwhile, the control samples were taken by rinsing the collector attached to the bottom of the cleaned nets with Milli-Q water. All samples were stored at 4 °C prior to analysis.

2.3. Sample analysis

2.3.1. Wet sieving

Water samples in the sampling bottle were poured through stacked stainless steel mesh sieves with mesh sizes of 5.0-mm and 0.3-mm, respectively. Residues on the 5.0-mm sieves were collected. Subsequently, the glass sampling bottles were rinsed and then filtered through the

Table 1
MPs sampling station, abundance, and chemical composition.

Sampling station	Sampling date	Longitude (E)	Latitude (N)	Number (0.3–5 mm)	Sampling area (m^2)	Abundance (items/km^2)	PE	PP	PA (nylon)	PVC	PS	Rubber	PET
CTRL-1	9/11/2017	146°29′51″	40°00′01″	9	3326.57	2705			9				
XTW3-6	8/28/2017	123°58′18″	20°59′32″	12	6700.51	1791	10	2					
XTW3-7	8/28/2017	125°58′51″	20°59′40″	17	1130.12	15,043	8	6			2	1	
XTW3-8	8/29/2017	127°59′25″	20°59′52″	5	2639.76	1894	5						
XTW3-9	8/30/2017	129°59′26″	20°59′59″	26	615.92	42,213	20	4		2			
XTW3-10	9/2/2017	139°59′45″	20°59′53″	42	1488.70	28,213	31	11					
XTJ1-19	9/4/2017	146°27′34″	20°59′35″	12	7574.48	1584	9	1	2				
XTJ1-14	9/6/2017	146°32′48″	26°59′43″	112	9030.00	12,403	91	20					1
XTJ1-6	9/9/2017	146°30′05″	34°57′42″	32	7645.99	4185	8	17	7				
XTJ1-4	9/10/2017	146°29′24″	36°59′42″	1	1561.83	640	1						
XTJ1-3	9/10/2017	146°31′22″	37°59′55″	3	4285.98	700	3						
XTJ1-2	9/11/2017	146°30′50″	38°59′24″	82	2427.90	33,774	43	37		1	1		
XTW2-5	9/15/2017	151°56′53″	35°01′30″	8	12,102.50	661	3	3				2	
XTW2-3	9/15/2017	150°00′17″	34°58′45″	9	4789.96	1879	5	3		1			
XTW2-1	9/16/2017	147°59′34″	35°00′30″	55	3628.54	15,158	8	45				2	
XTW3-5	9/24/2017	119°58′24″	21°01′25″	10	8976.62	1114	7	3					
XTW3-4	9/24/2017	119°29′21″	20°59′49″	44	4600.00	9565	14	28		2			
XTW3-3	9/24/2017	118°59′25″	21°00′30″	52	3596.22	14,460	41	11					
Total				531		187,982	307	191	18	6	3	5	1
Percentage (%)							57.8%	36.0%	3.4%	1.1%	0.6%	0.9%	0.2%

sieves with Milli-Q water. Salt was also removed from the field samples during this process. This procedure was repeated three times to ensure complete removal of samples from the bottle. Then the 0.3-mm sieve was rinsed thoroughly with Milli-Q water and all the material collected was transferred to clean beakers. Finally, the sample in the beaker was dried in the oven at 75 °C.

2.3.2. Digestion

20 mL aqueous 0.05 M Fe(II) solution was first added to the dried beaker containing the 0.3 mm size fraction of the collected solids, and then 20 mL 30% H_2O_2. The mixture covered with a watch glass was kept at room temperature for 5 min and then heated at 75 °C on a hotplate under the hood until bubbles appeared. The beaker was removed and kept until the reaction is completed. Subsequently, it was heated at 75 °C for another 30 min. Another 20 mL 30% H_2O_2 was added and the above process is repeated to ensure a thorough oxidation of organic matters.

2.3.3. Density separation

About 6 g NaCl was added to a 20 mL sample to increase the density of the solution. The mixture was transferred to a glass funnel after the complete dissolution of NaCl (~300 g L^{-1}). The beaker was rinsed several times with Milli-Q water to ensure that the solid was completely transferred to a density separator which was loosely covered with an aluminum foil and settled overnight. Most plastics would float to the surface the next day. Further MPs screening was conducted through a visual inspection of any settled solids. The identified MPs were drained and collected using forceps. The supernatant was filtered through a glass fiber filter (GF/F Whatman, 47 mm diameter and 0.7 μm pore size) using a vacuum system. The funnel was rinsed several times with Milli-Q water and the solution was poured through the glass fiber filter as well. Finally, all solids including the suspected MPs in the settled solids from the filter were collectively placed in a clean petri dish covered with aluminum foil and air dried overnight for further analysis to obtain the type, abundance, shape, color, and size of MPs.

2.4. Visual identification

The collected solids were further inspected visually under a microscope (Olympus CKX 41, Japan) for MPs screening. The composition of discernable solids was identified using Micro-Raman spectroscopy.

2.5. Chemical classification

Micro-Raman Spectroscopic analysis was conducted using a Senterra II Compact Raman Microscope (Bruker Optics Inc., Billerica, MA) coupled with an optical microscope with a grafting of 1200 lines/mm with 20× and 50× objectives (Infinity, USA). All the MPs samples were excited with visible 532 nm and near-infrared 785 nm diode lasers of 1–60 mW focused onto the sample for 10–60 s. Raman spectra were recorded as line measurements (>4 points) on various parts of the focused particle to avoid any contamination of impurities. All spectra with a frequency resolution of ~3–5 cm^{-1} and range of 400–4000 cm^{-1} were analyzed using the OPUS 7.5 software (Opus software Inc., San Rafael, CA). Both commercial library and self-created library references of main plastic polymers (Table S2) were adopted for identifying the composition of MPs.

2.6. Surface morphology

The samples were coated 3 nm layer of Au using a sputter coating system (Leica EM ACE200, Germany) to enhance their conductivity. The surface topography and element analysis of MPs were conducted by a SEM unit (Zeiss EVO 18, Germany) with an energy dispersive X-ray analysis (EDS) system, which are controlled by the SmartSEM® software operated via a graphical user interface and Aztec One software, respectively.

2.7. Physical oceanography parameters

Oceanography parameters including temperature, conductivity, and pressure were measured using a SBE 917 Plus CTD (Sea-Bird Scientific, USA). The sea state was measured using a vessel-mounted Acoustic Doppler Current Profiler (ADCP) and the automatic weather reporting system operated by the Marine Technology Center, State Oceanic Administration of China. The sea state parameters, such as wind speed, wind direction are listed in Table S1 in the Supporting Information (SI). The vertical distribution of MPs concentration is more closely related to wind-driven and wave-induced mixing. As pointed by Kukulka et al. (2012), the MPs concentration at surface and subsurface is correlated with wind speed through wind-induced mixing. However, we only collected MPs samples at the surface in this study. Therefore, the effect of wind speed on the vertical distribution of MPs is not well resolved in the present measurements.

The underway current was measured by a vessel-mounted Acoustic Doppler Current Profiler (ADCP). Maps of surface dynamic topography were derived from the satellite altimetry data from AVISO website (https://www.aviso.altimetry.fr/en/home.html) and the deduced absolute geostrophic velocities. The global daily sea surface temperature (SST) data was given by global high-resolution SST remote sensing.

3. Results and discussion

3.1. Abundance

The surface abundance of MPs at 18 stations in the Northwestern Pacific is illustrated in Fig. 1. MPs are present at all stations, suggesting the pervasiveness of MPs pollution in the Northwestern Pacific. A total of 531 counts of MPs were detected at the 18 stations across the pelagic zone during the field survey. The concentration of MPs differs significantly among 18 stations. Fig. 2 shows that the MPs abundance at the ocean surface ranges from 6.4×10^2 to 4.2×10^4 items·km^{-2}, which is represented by the size of pie charts in Fig. 1 with a median and mean value of 3.4×10^3 and 1.0×10^4 items·km^{-2}. Approximately 39% of the observed MPs abundance is over 1.0×10^4 items·km^{-2}. MPs accumulation is visible west of the Luzon Strait and changes from 1.1×10^3 items·km^{-2} in the east to 1.4×10^4 items·km^{-2} in the west as shown in Fig. 1. We believe that MPs were conveyed to and accumulated at XTW3-3, located at the west side of the Luzon Strait by the westward intrusion of the Kuroshio Current into the South

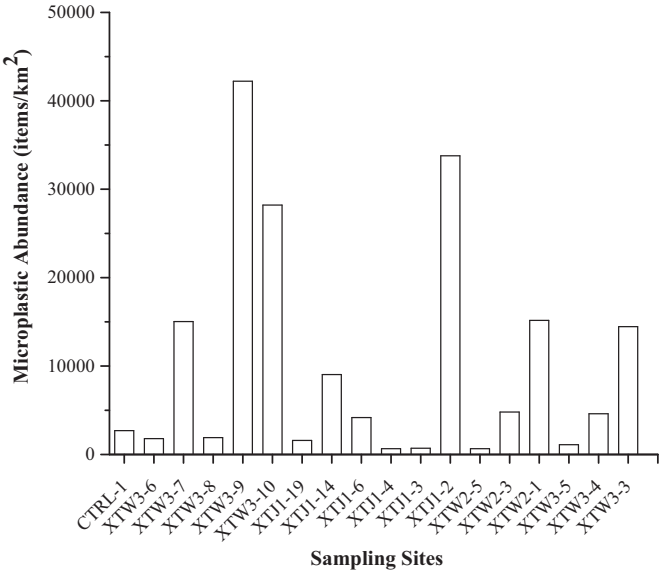

Fig. 2. Microplastic abundance observed at 18 field stations in the Northwestern Pacific.

Table 2
MPs abundances of sea surface waters across the world.

Location	Time	Sampling method	MPs abundance (items km^{-2})	References
Arabian Bay	December 2014–March 2015	Surface neuston net (300 μm)	4.4×10^4–1.5×10^6	(Abayomi et al., 2017)
Arctic Ocean	June 5–15, 2014	Manta net (330 μm)	2.8×10^4	(Lusher et al., 2015)
South Pacific Ocean	March 23–April 21, 2011	Manta trawl (330 μm)	0–4.0×10^5	(Eriksen et al., 2013)
East Asian seas around Japan	July 17–September 2, 2014	Neuston net (350 μm)	1.7×10^6	(Isobe et al., 2015)
Western North Atlantic Ocean		Surface plankton net tows (330 μm)	0–5.8×10^5	(Law et al., 2010)
Caribbean Sea	1986–2008		$1.4 \times 10^3 \pm 1.1 \times 10^2$[a]	
Gulf of Maine			$1.5 \times 10^3 \pm 2.0 \times 10^2$[a]	
Mediterranean	July 9–August 6, 2010	Manta trawl (330 μm)	0–9.0×10^5	(Collignon et al., 2012)
Northeastern Pacific Ocean	August–September 2012	Saltwater intake system of the vessel	8 to 9.2×10^3 (items/m^3)	(Desforges et al., 2014)
Kuroshio Current area	April 2000–April 2001	Surface neuston net (330 μm)	$1.7 \times 10^5 \pm 4.7 \times 10^5$[a]	(Yamashita and Tanimura, 2007)
Northwestern Pacific Ocean	August 25 to September 26, 2017	Manta trawl (330 μm)	6.4×10^2–4.2×10^4	This study

[a] Average ± standard deviation.

China Sea through the Luzon Strait. This current is mainly generated by the wind stress curl off the southwest Taiwan (Yuan et al., 2014). At the east of the Luzon Strait, the MPs abundance increases from 1.8×10^3 items·km^{-2} to 4.2×10^4 items·km^{-2} in the eastward direction. The relatively high MP abundance at the XTJ1-2 may be attributed to its geographic proximity to the densely populated coastlines and industrialized Japanese coast of Pacific. Dynamic human activities along the Japan coast of Pacific increase the terrestrial effluents of plastic debris into the ocean. The station XTW3-9 has the highest MP abundance of 4.2×10^4 items·km^{-2} (Fig. 2). Particularly high MP concentrations have been reported in the convergent zones of subtropical ocean gyres due to accumulation and persistence of MPs in these regions (Cózar et al., 2014; Eriksen et al., 2014; Mauro et al., 2017; Moore et al., 2001). As shown in Fig. 5, station XTW3-9 is located close to an ocean current gyre.

There are no standardized sample acquisition protocols to monitor MPs. Different sampling gears (e.g., plankton trawls, neuston nets, bongo nets, manta trawls) with various mesh sizes have been adopted in previous studies. Therefore, various units for MPs abundance (e.g., items m^{-2}, items m^{-3}, g m^{-2}, items kg^{-1} sediment, etc.) have been utilized. Inconsistency in the sampling approach, extraction technique, and reporting unit makes it difficult to compare MPs measurement results. Table 2 shows comparisons of our field survey results with other studies with similar sampling methods and reporting units. Our observed MPs abundance is at least one order of magnitude smaller than that at the Arabian Bay observed by Abayomi et al. (2017). This may be due to the fact that the Arabian Bay is a marginal sea bordering the Indian Ocean and receives more plastic debris from the land. Also, the enclosed ecosystem in the Arabian Bay has a limited exchange with the pelagic zones, therefore, subject to accumulation of MPs close to the coast in the bay (Mauro et al., 2017). Similar to Arabian Bay, the Mediterranean Sea is a semi-enclosed ocean surrounded by continents, which discharge large amounts of plastic debris into the ocean, therefore, has a relatively high MP abundance (Table 2). The mean MPs abundance in the South Pacific Ocean and Western North Atlantic Ocean is about one order of magnitude higher than that observed during our field survey in the Northwestern Pacific (Table 2). The MPs level in the East Asian sea around Japan is even higher (1.7×10^6 items km^{-2}, Table 2) (Isobe et al., 2015), about 50 times what we observed in the Northwestern Pacific. Again, this may be due to the proximity of the East Asian seas to the highly urbanized and industrialized land. Furthermore, relatively high averaged MP abundance (1.7×10^5 items km^{-2}, Table 2) was identified in the Kuroshio Current region indicated by the arrow in Fig. 1, suggesting that the Kuroshio Current plays an important role in transporting and retaining plastics from nearby terrestrial sources.

3.2. Chemical fingerprints

Fig. 3 shows the distinct Micro-Raman spectral characteristics for plastic polymers that can be used as reference spectra to identify the composition of this type of MPs. Fig. 4 shows the Micro-Raman spectra for selected samples of MPs with various color, shape and type collected from the Northwestern Pacific. The MP polymer type was determined by matching the characteristic peaks of recorded Micro-Raman spectra (Fig. 4) with the reference spectra of known plastics illustrated in Fig. 3. Overall, seven conventional plastic polymers (PE, PP, PA, PVC, PS, rubber, and PET) were detected in our field survey samples. PE accounted for the largest proportion of MPs (~58%), followed by PP (36%) and PA (3%). The Micro-Raman spectral results show that PE and PP are the two predominant plastic polymers in our MPs samples, consistent with earlier findings (Cózar et al., 2014; Ghosal et al., 2017; Hidalgo-Ruz et al., 2012).

Identifying the type of MPs provides clues about their origins. For example, chemical compositions of MPs at the same latitude of 21°N from 123°E to 146°E are comparable, with 83% PE and 17% PP, 77% PE and 15% PP, 74% PE and 26% PP, and 81% PE and 18% PP for sample stations XTW3-6, XTW3-9, XTW3-10, and XTJ1-14, respectively (Fig. 1). The MPs in the east stations may originate from the neighboring land-based regions. Unlike the stations mentioned above at 21°N, the major MPs in the stations adjacent to Japan (e.g., XTJ1-2, XTJ1-6, XTW2-1, etc.) is PP. The MPs sample at XTJ1-6 and XTW2-1 consists 25% PE and 53% PP, 15% PE and 82% PP, respectively. The large variations in the MPs compositions are due to the large variations in the origin of MPs. Due to the geographic proximity to Japan, MPs at these stations are

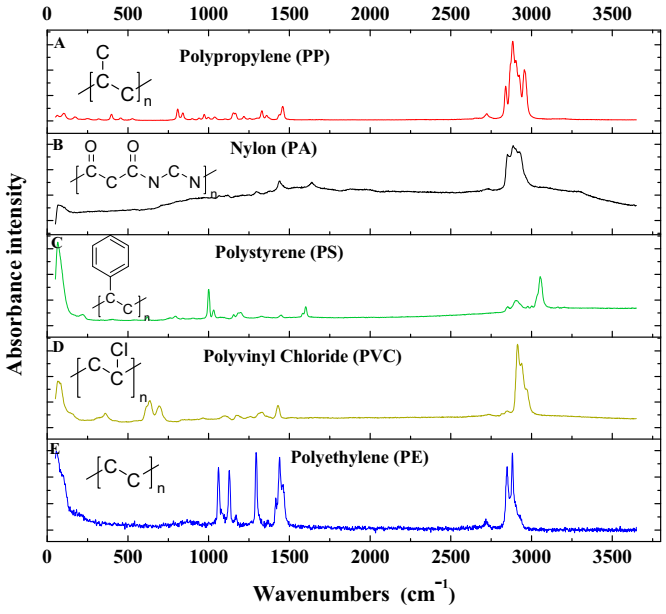

Fig. 3. Micro-Raman spectra of common virgin plastic polymers. A: Polypropylene (PP); B: nylon (PA); C: polystyrene (PS); D: polyvinyl chloride (PVC); E: polyethylene (PE).

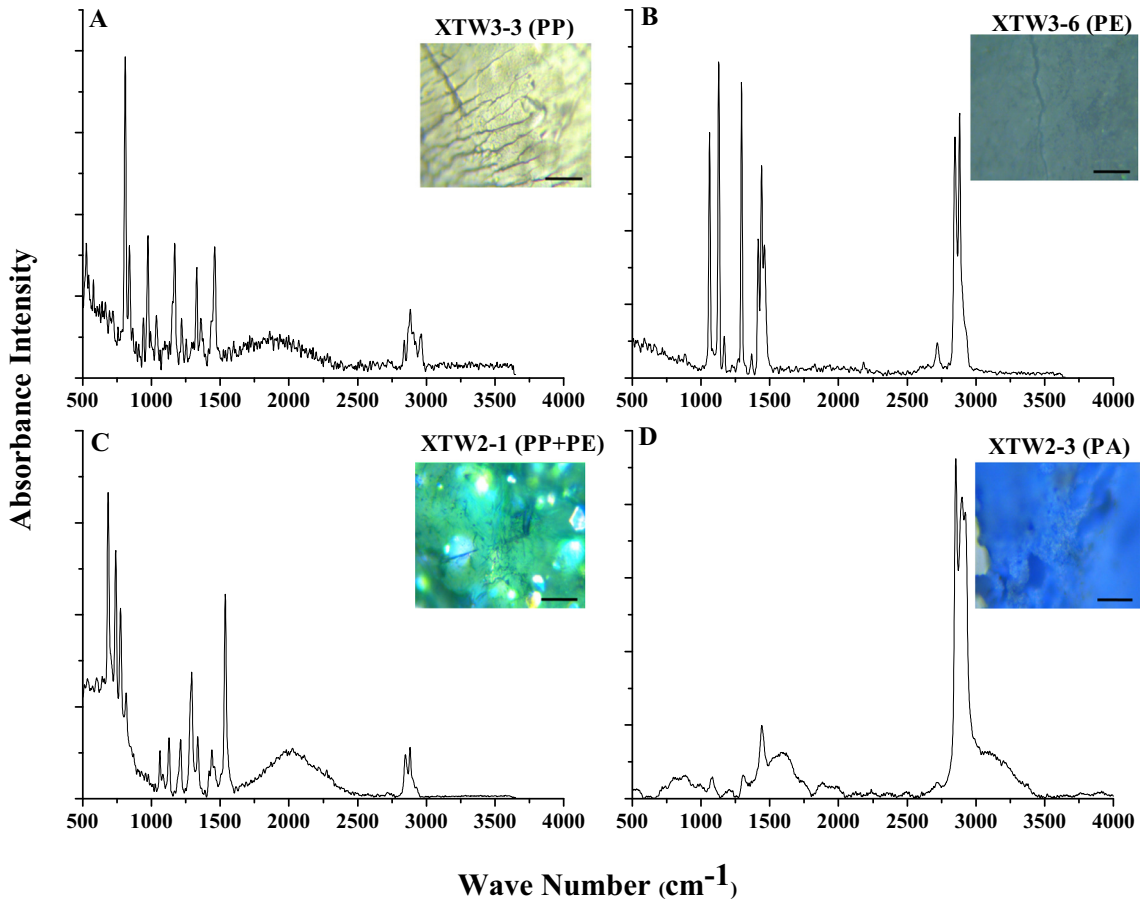

Fig. 4. Micro-Raman spectra of selected MPs samples. A: XTW3-3, PP, transparent film; B: XTW3-6, PE, white sheet; C: XTW2-1, PP + PE, green bulk; D: XTW2-3, nylon, blue ball. Scale bar = 20 μm.

likely originated from the coast of Japan. In addition, the MPs at the sampling station XTJ1-2 are composed of comparable fractions of PE (52%, Table 1) and PP (45%, Table 1), which is in good agreement with the latest statistics report of plastics production materials in 2016–2017 provided by the Japan Plastics Industry Federation. According to that report, similar amounts of PE and PP materials (4.53 and 4.37 million tons, respectively) were produced from January 2016 to September 2017 (JPIF, 2017). These results suggest that the Pacific coast of Japan may be the geographic origin of the marine plastic debris in the Northwestern Pacific. However, future work is required to further verify this hypothesis.

3.3. Spatial patterns

Physical oceanographic parameters, including vessel-mounted ADCP measurements of underway current, satellite altimetry data, and sea surface temperature were analyzed to examine the mechanisms for the MPs distribution patterns in the studied area. Fig. 5 illustrates the Kuroshio and the Kuroshio Extension in the Northwestern Pacific. A large-scale recirculation gyre is formed at the southeast of the Kuroshio adjacent to the coast of Japan (130.7–136.0°E). The Kuroshio Extension path south of Japan oscillates southeastward and northeastward in a meandering manner, resulting in a double gyre (141–151°E) centered around (143.10°E, 36.35°N) and (149.19°E, 36.41°N). During the survey, the observed anomaly of Southern Recirculation Gyre south of the Kuroshio Extension manifested as two warm eddies at relatively stable locations, south of the eddy centers. Fig. 5 also shows the presence of numerous mesoscale eddies in the east of the Kuroshio and south of the Kuroshio Extension, where multiple MP sampling stations (e.g., XTW3-6, XTJ1-2, XJT1-6, XTW2-1, Fig. 1) are located. Ocean circulation in this area is closely linked to the intensity and trajectory of these mesoscale eddies which therefore influences the abundance and spatial distribution of MPs in this region. For example, the intensive warm eddy east of the Kuroshio near Taiwan (21.9–25°N) in Fig. 5 would modulate the MPs transport at the nearby field stations such as XTW3-6.

The overall flow direction at the latitude range of 21–30°N is between northeastward and northward. The transect of 21.8–24.3°N has a flow velocity >30 cm s^{-1} near the warm eddy and the confluence of cold and warm eddies leads to an intensive current of 88.80 cm s^{-1} around 146.50°E, 22.41°N. The overall northeastward directed currents with higher velocity south of 24.3°N may carry MPs towards the northeast, and cause the relatively high MPs abundance at the station XTJ1-14. In addition, the source-specific distribution may be obtained based on the subtle differences in the MP chemical fingerprints along XTW3-5, XTW3-6, XTW3-7, XTW3-9, XTW3-10, and XTJ1-14 (Fig. 1).

The transect of 34.6–36.4°N passed through the Kuroshio Extension path with a strong northeastward current. The maximum current velocity of 188.90 cm s^{-1} in the northeastward direction was observed at the Kuroshio extension path near (146.54°E, 35.73°N) as shown in Fig. 5, which carry the MPs northeastward towards the XTW 2-1 at (147.59°E, 35.00°N). This explains the observed higher MPs abundance (1.5×10^4 items km^{-2}) at the station XTW2-1 than its neighboring station XJT1-6. The transect of 36.4–37.8°N is located near the south edge of a warm eddy north of the Kuroshio Extension (cf. Fig. 5) with a steady southwestward flow. The transect of 37.8°N passes by the warm eddy (Fig. 5) with a stable southeastward current. Fig. 5 shows that ocean current south of the Kuroshio Extension (south of 34°N) is distinctly weaker than that north of the Kuroshio Extension. The northward

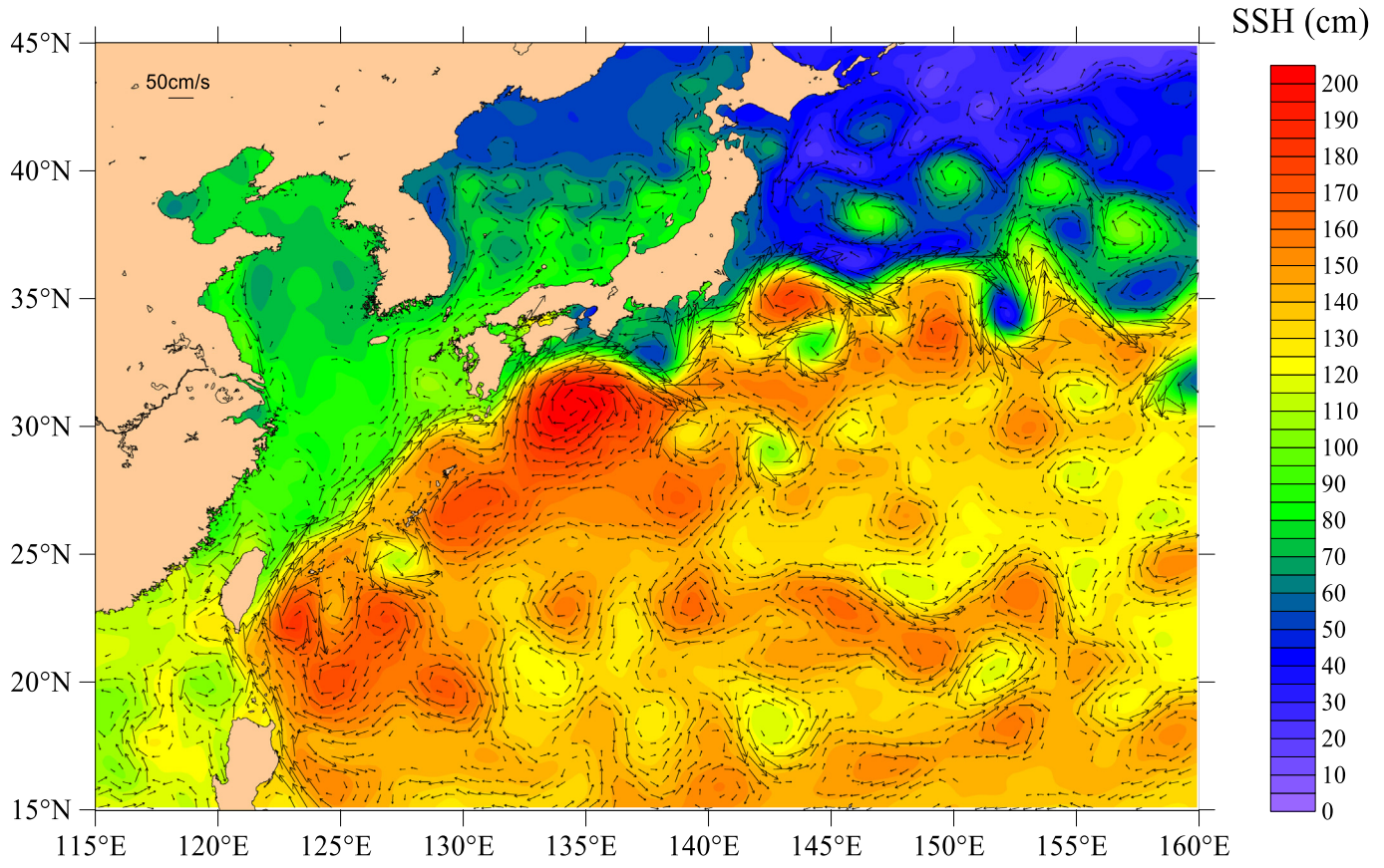

Fig. 5. Map of ocean surface dynamic topography (color) and geostrophic currents (arrows) in the present study area from Aug 25–Sep 26, 2017. Note that current <10 cm s^{-1} is excluded from this figure.

current with a relative higher magnitude in the north implies that the MPs influx from the Japanese coast may travel northward rather than accumulate in the south of the Kuroshio Extension. This circulation pattern is consistent with our observation that the MPs abundance in the stations XTJ1-6, XTW2-1 south of the XTJ1-2 is relatively lower than that at XTJ1-2 (Fig. 1).

3.4. Size

Microplastic size was analyzed using the method developed by the National Oceanic and Atmospheric Administration (NOAA, 2015). Our analysis results show that the size of ~50% of the detected MPs spans from 0.5 to 1.0 mm. 29.8% of MPs are medium size (1–2.5 mm), while 17.6% of MPs are large size (2.5–5.0 mm) (cf. Fig. 6A). Our observations are consistent with the recent findings that relatively small size of particles dominates in the MPs (Isobe et al., 2015; Isobe et al., 2017; Song et al., 2014; Zhang et al., 2017). The proportion of MPs of certain size increases with decreasing particle size. It was proposed that the plastic aging process and weather forcing help to break large marine plastic debris into small fragments, resulting in a decrease in the size of MPs (Isobe, 2016).

3.5. Color

A wide spectrum of colors was observed for the MPs during our field survey. Fig. 6B indicates that the dominant color of MPs in the Northwestern Pacific is white (~57.4%), followed by transparent (22.8%), green (6.6%), black (6.4%), blue (2.8%), yellow (2.4%), and purple (1.5%). Note that the pale MPs (white and transparent) accounts for 80.2% of the observed MPs, whereas the other colors are <20%. Our findings agree well with previous findings that the translucent and light colored floating marine debris account for 94% of all MPs in the Sargasso Sea (Carpenter et al., 1972), 82–89% in the South Atlantic (Ryan et al., 2009), and 72% in the North Pacific (Day et al., 1985). The large variety of colors for MPs implies that MPs may have colors similar to natural marine food, therefore, may confuse natural prey and predator behaviors and lead to color-specific ingestion by marine biota (Wright et al., 2013b). For instance, some visual predators may mistake MPs of similar physical appearance (e.g., white, tan, and yellow plastics) as food (Wright et al., 2013b).

Color has also been recognized as a good indicator of residence time at the ocean surface and degree of weathering (Rodríguez-Seijo and Pereira, 2016). The degree of yellowing or darkening is largely due to the increased carbonyl index, therefore the extent of aging or degradation (Stolte et al., 2015). In lieu of bright and fresh colors, nearly all the observed MPs from our field survey displays dull and faded hues, which indicates that they were transported across the ocean and underwent various aging processes, e.g. weathering and degradation over a long period of time. This result is consistent with the previous finding that the discoloration of the plastic polymer is the visual indicator of degradation (Gewert et al., 2015).

3.6. Shape

Fig. 6C shows that the MPs in the Northwestern Pacific has a broad range of irregular shapes, including fragments, lines, granules and films. Granules account for 39.7% of all our collected MPs samples. Sheets, films, and lines represented 26.7%, 24.7%, and 8.9% of the MPs respectively. The shape of MPs may be affected by (1) the initial form of primary plastics, (2) surface degradation and erosion processes such

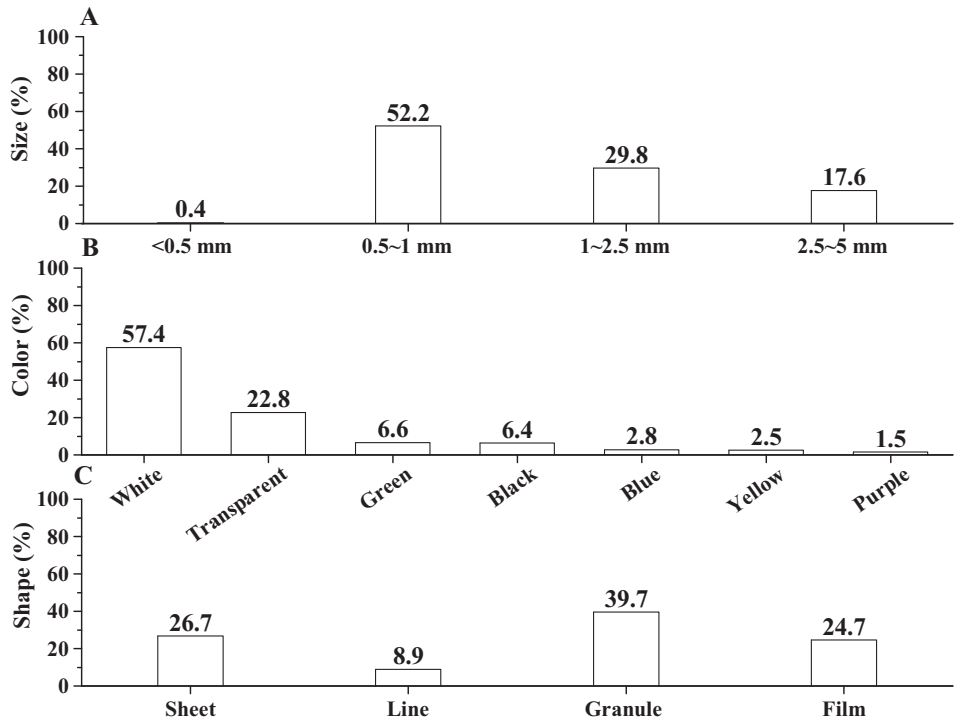

Fig. 6. Histogram distributions of A: size; B: color; C: shape of MPs.

as mechanical abrasion, photodegradation and biological activities, (3) residence time at the sea. Surface roughness, cracks, and brittleness are also good indicators of residence time. Sharp edges may suggest a short residence time of plastics, whereas smooth ones may indicate that the MPs have resided at the sea for an extended time of period (Hidalgo-Ruz et al., 2012; Rodríguez-Seijo and Pereira, 2016). However, smooth/rough edges may not be a good proxy for plastic age in some cases. For example, brand new resin pellets possess smooth surfaces, but they are not the aged plastic particles. In addition, plastics do not weather in the same manner as rocks or sediments.

Previous studies showed that the origins and pathways of MPs may be inferred based on their shapes (Cheung and Fok, 2016; Lenz et al., 2015; Murray and Cowie, 2011). For instance, lines (fibers) are an indication of sewage sources (Browne et al., 2011) and prevail in the near shore region (Cózar et al., 2014). Line MPs occasionally appear in the open sea after a long migration from continents. Our field survey results reveal that <10% of MPs are lines in the Northwestern Pacific, while the majority of MPs are sheets, granules, and films (Fig. 6C) in this region. The relatively low content of lines observed by our field survey is due to the fact that our study area is located in the pelagic zone, far away from the land. The majority of MPs pervasive in the remote ocean are fragments of larger plastic debris. Accordingly, our field survey data shows that fragments such as sheets and films account for ~51.4% of the total MPs.

3.7. Surface morphology

Fig. 7 shows the SEM images for the surface morphology of selected MPs. By comparisons with virgin plastic polymers, the SEM images of surface roughness, cracks, and brittleness are evidence of the aged MPs surfaces and edges from their transport and residence at the sea. Fig. 7A shows transparent particles are filled with cracks. Fig. 7B illustrates a green sheet with a netlike structure full of bumps and hollows. Fig. 7C indicates a white ball with apparent hollows, while Fig. 7D shows a MP ruptured as pronounced transverse and longitudinal cracks developed on the surface of the green fragment. Weathering, photodegradation, prolonged physical wearing, or biological activity may contribute to the evolution of surface topography of MPs during their journey across the ocean (Andrady et al., 1998; Corcoran et al., 2009; Morét-Ferguson et al., 2010). The increased surface roughness may affect the biofilm formation on the surface of MPs. Nauendorf et al. (2016) reported that the surface roughness influences microbial colonization more than surface wettability. Verran and Boyd (2001) also stated that the surface roughness plays an important role in bio-attachment processes (Verran and Boyd, 2001). Furthermore, surface cracking increases the exposure of the interior plastic structure to the environment, so that MPs are more vulnerable to further decomposition, embrittlements and disintegrations over time (Vasile and Dekker, 2000). Based on these findings, a large number of very small MPs (e.g., nanoscale plastic particles) may be generated from the breakdown of large pieces of plastics, nonetheless, these countless plastic particles were not considered in this study due to the methodological constraints.

Our element analysis revealed that strong nitrogen peaks appear on the surface of all MPs samples for EDS measurements (Tables S3–S6). Nitrogen is not a constituent of virgin plastic polymers except for nylon, such as polyethylene, polypropylene and polystyrene. The Micro-Raman spectroscopic analysis further confirmed that these MPs were primarily composed of PE and PP rather than nylon. Based on these results, we choose nitrogen as a proxy for biomass. The pervasive occurrence of nitrogen in the sampled MPs is an indicator of bioaccumulation, consistent with earlier studies (Law et al., 2010; Morét-Ferguson et al., 2010). Nonetheless, we found that biofilms were formed on the surface of MPs samples processed through H_2O_2 digestion, as indicated by the presence of nitrogen (Tables S3–S6) and the attachments of biomass (Fig. S1). These results suggest the strong interactions between MPs and biota.

4. Conclusions

Field observations of Microplastics (MPs) in the Northwestern Pacific Ocean were conducted to investigate the abundance, chemical

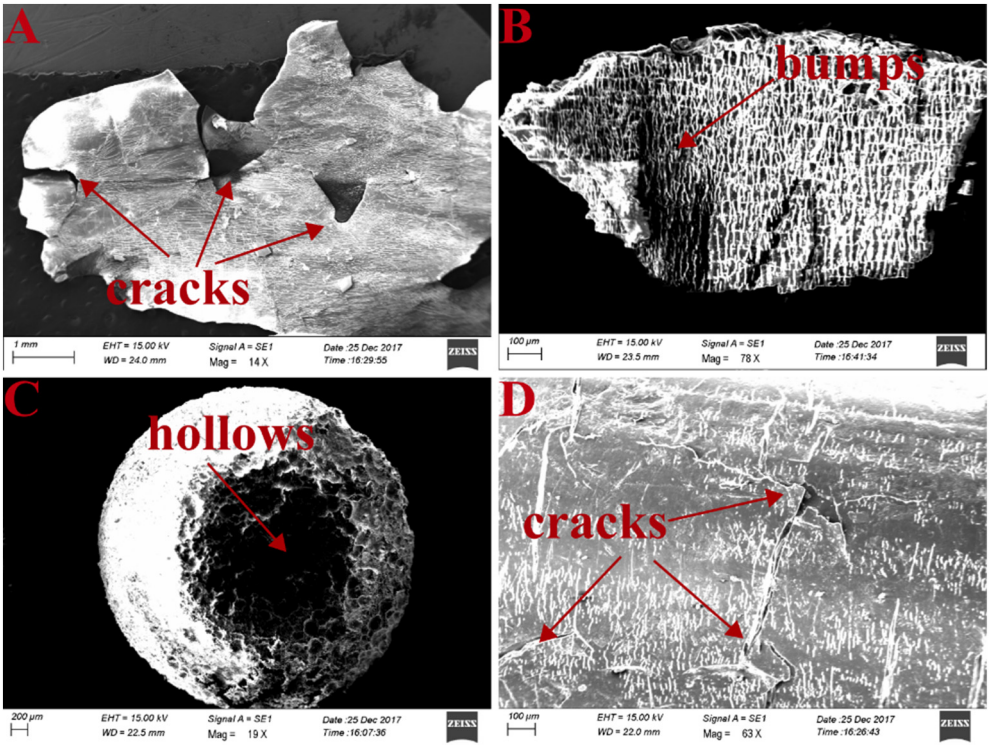

Fig. 7. The scanning electron microscope (SEM) images of MPs surface morphology of representative samples. A: Transparent film (polyethylene, PE); B: green sheet (polyethylene + polypropylene, PE + PP); C: white ball (polyethylene, PE); D: green fragment (polypropylene, PP).

composition, spatial pattern, color, shape, and surface morphology of MPs and to provide new insights for the potential sources, pathways, distributions and generation mechanisms of MPs in the pelagic zone. Our observation results indicated the pervasiveness of MPs in the open ocean surface with an average abundance of 1.0×10^4 items km^{-2}. The Micro-Raman spectroscopic analysis results indicate that the major compositions of MPs are polyethylene (57.8%), polypropylene (36.0%) and nylon (3.4%). The chemical fingerprints of MPs at stations XTW3-5, XTW3-6, XTW3-7, XTW3-9, XTW3-10, and XTJ1-14 are similar to each other, which indicates that the origin of the MPs at these stations are the same, namely, the nearby land in Philippines, Taiwan, and China Mainland. In contrast, the major composition of MPs at the stations adjacent to Japan, XTJ1-2, XTJ1-6 and XTW2-1, is polypropylene, which indicates that the sources of the MPs are different for this region, namely, the Japanese coast. Our observations indicate that 52.2% of the MPs are between 0.5 and 1.0 mm in size, 39.7% of the MPs are granules in shape and 80.2% of the MPs are white and transparent color. The observed underway current and sea surface temperature by vessel-mounted ADCP and CDT, satellite altimetry data, and the chemical fingerprints of MPs, indicate that the spatial distribution of MPs is attributed to the combined effects of ocean circulation pattern, adjacent eddies, the Kuroshio and Kuroshio Extension. Our observational results provided a holistic view of the abundance, distribution, and characteristics of MPs in the Northwestern Pacific Ocean. This would improve the assessments and mitigations of the hazards and risks posed by MPs to the marine environment and human health.

Acknowledgements

This work was supported by grants from the Eastern Pacific Eco-environment Monitoring and Protection Project (DY135-E2-5-02); State Oceanic Administration of China Special Fund Project (SOA201303); the 45th Chinese COMRA Cruise. Oceans & Fisheries Bureau of Xiamen, China (Contract No. 14PST63NF27).

Appendix A. Supplementary data

MPs sampling sites, sample processing, EDS results, supporting tables and figures referenced in this study. Supplementary data to this article can be found online at doi: https://doi.org/10.1016/j.scitotenv.2018.09.244.

References

Abayomi, O.A., Range, P., Al-Ghouti, M.A., Obbard, J.P., Almeer, S.H., Ben-Hamadou, R., 2017. Microplastics in coastal environments of the Arabian Gulf. Mar. Pollut. Bull. 124, 181–188.
Andrady, A.L., Neal, M.A., 2009. Applications and societal benefits of plastics. Philos. Trans. R. Soc. Lond. 364, 1977–1984.
Andrady, A.L., Hamid, S.H., Hu, X., Torikai, A., 1998. Effects of increased solar ultraviolet radiation on materials. J. Photochem. Photobiol. B Biol. 46, 96–103.
Auta, H.S., Emenike, C.U., Fauziah, S.H., 2017. Distribution and importance of microplastics in the marine environment: a review of the sources, fate, effects, and potential solutions. Environ. Int. 102, 165–176.
Bakir, A., Rowland, S.J., Thompson, R.C., 2012. Competitive sorption of persistent organic pollutants onto microplastics in the marine environment. Mar. Pollut. Bull. 64, 2782–2789.
Barnes, D.K.A., Galgani, F., Thompson, R.C., Barlaz, M., Heap, B., 2009. Accumulation and fragmentation of plastic debris in global environments. Philos. Trans. R. Soc. Lond. Ser. B Biol. Sci. 364, 1985–1998.
Bergmann, M., Gutow, L., Klages, M., 2015. Marine Anthropogenic Litter. Springer, p. P204.
Bergmann, M., Wirzberger, V., Krumpen, T., Lorenz, C., Primpke, S., Tekman, M.B., et al., 2017. High quantities of microplastic in arctic deep-sea sediments from the HAUSGARTEN observatory. Environ. Sci. Technol. 51, 11000–11010.
Brennecke, D., Duarte, B., Paiva, F., Caçador, I., Canning-Clode, J., 2016. Microplastics as vector for heavy metal contamination from the marine environment. Estuar. Coast. Shelf Sci. 178, 189–195.
Browne, M.A., Dissanayake, A., Galloway, T.S., Lowe, D.M., Thompson, R.C., 2008. Ingested microscopic plastic translocates to the circulatory system of the mussel, *Mytilus edulis* L. Environ. Sci. Technol. 42, 5026–5031.
Browne, M.A., Crump, P., Niven, S.J., Teuten, E., Tonkin, A., Galloway, T., et al., 2011. Accumulation of microplastic on shorelines worldwide: sources and sinks. Environ. Sci. Technol. 45, 9175–9179.
Carpenter, E.J., Anderson, S.J., Harvey, G.R., Miklas, H.P., Peck, B.B., 1972. Polystyrene spherules in coastal waters. Science 178, 749–750.
Cauwenberghe, L.V., Vanreusel, A., Mees, J., Janssen, C.R., 2013. Microplastic pollution in deep-sea sediments. Environ. Pollut. 182, 495–499.

Cauwenberghe, L.V., Devriese, L., Galgani, F., Robbens, J., Janssen, C.R., 2015. Microplastics in sediments: a review of techniques, occurrence and effects. Mar. Environ. Res. 111, 5–17.

Cheung, P.K., Fok, L., 2016. Evidence of microbeads from personal care product contaminating the sea. Mar. Pollut. Bull. 109, 582–585.

Cole, M., Lindeque, P., Fileman, E., Halsband, C., Galloway, T.S., 2015. The impact of polystyrene microplastics on feeding, function and fecundity in the marine copepod *Calanus helgolandicus*. Environ. Sci. Technol. 49, 1130–1137.

Collignon, A., Hecq, J.H., Glagani, F., Voisin, P., Collard, F., Goffart, A., 2012. Neustonic microplastic and zooplankton in the North Western Mediterranean Sea. Mar. Pollut. Bull. 64, 861–864.

Corcoran, P.L., Biesinger, M.C., Grifi, M., 2009. Plastics and beaches: a degrading relationship. Mar. Pollut. Bull. 58, 80–84.

Cózar, A., Echevarría, F., Gonzálezgordillo, J.I., Irigoien, X., Ubeda, B., Hernándezleón, S., et al., 2014. Plastic debris in the open ocean. Proc. Natl. Acad. Sci. U. S. A. 111, 10239–10244.

Day, R.H., Wehle, D.H., Coleman, F.C., 1985. Ingestion of plastic pollutants by marine birds. Proceedings of the Workshop on the Fate and Impact of Marine Debris. 2. US Dep. Commer. NOAA Tech Memo NMFS Honolulu, Hawaii, pp. 344–386.

Desforges, J.P., Galbraith, M., Dangerfield, N., Ross, P.S., 2014. Widespread distribution of microplastics in subsurface seawater in the NE Pacific Ocean. Mar. Pollut. Bull. 79, 94–99.

Eriksen, M., Maximenko, N., Thiel, M., Cummins, A., Lattin, G., Wilson, S., et al., 2013. Plastic pollution in the South Pacific subtropical gyre. Mar. Pollut. Bull. 68, 71–76.

Eriksen, M., Lebreton, L.C., Carson, H.S., Thiel, M., Moore, C.J., Borerro, J.C., et al., 2014. Plastic pollution in the world's oceans: more than 5 trillion plastic pieces weighing over 250,000 tons afloat at sea. PLoS One 9, e111913.

Gewert, B., Plassmann, M.M., Macleod, M., 2015. Pathways for degradation of plastic polymers floating in the marine environment. Environ. Sci. Process. Impact 17, 1513–1521.

Ghosal, S., Chen, M., Wagner, J., Wang, Z.M., Wall, S., 2017. Molecular identification of polymers and anthropogenic particles extracted from oceanic water and fish stomach - a Raman micro-spectroscopy study. Environ. Pollut. https://doi.org/10.1016/j.envpol.2017.10.014.

Hamlin, H.J., Marciano, K., Downs, C.A., 2015. Migration of nonylphenol from food-grade plastic is toxic to the coral reef fish species *Pseudochromis fridmani*. Chemosphere 139, 223–228.

Hidalgo-Ruz, V., Gutow, L., Thompson, R.C., Thiel, M., 2012. Microplastics in the marine environment: a review of the methods used for identification and quantification. Environ. Sci. Technol. 46, 3060–3075.

Isobe, A., 2016. Percentage of microbeads in pelagic microplastics within Japanese coastal waters. Mar. Pollut. Bull. 110, 432–437.

Isobe, A., Uchida, K., Tokai, T., Iwasaki, S., 2015. East Asian seas: a hot spot of pelagic microplastics. Mar. Pollut. Bull. 101, 618–623.

Isobe, A., Uchiyama-Matsumoto, K., Uchida, K., Tokai, T., 2017. Microplastics in the Southern Ocean. Mar. Pollut. Bull. 114, 623–626.

Jambeck, J.R., Geyer, R., Wilcox, C., Siegler, T.R., Perryman, M., Andrady, A., et al., 2015. Plastic waste inputs from land into the ocean. Science 347, 768–771.

JPIF, 2017. Statistics of The Japan Plastics Industry Federation. Available from:. http://jpif.gr.jp/english/statistics/index.html.

Kooi, M., Van Nes, E.H., Scheffer, M., Koelmans, A.A., 2017. Ups and downs in the ocean: effects of biofouling on the vertical transport of microplastics. Environ. Sci. Technol. 51, 7963–7971.

Kukulka, T., Proskurowski, G., Morét-Ferguson, S., Meyer, D.W., Law, K.L., 2012. The effect of wind mixing on the vertical distribution of buoyant plastic debris. Geophys. Res. Lett. 39, 7601.

La Daana, K.K., Officer, R., Lyashevska, O., Thompson, R.C., O'Connor, I., 2017. Microplastic abundance, distribution and composition along a latitudinal gradient in the Atlantic Ocean. Mar. Pollut. Bull. 115, 307–314.

Law, K.L., MorétFerguson, S., Maximenko, N.A., Proskurowski, G., Peacock, E.E., Hafner, J., et al., 2010. Plastic accumulation in the North Atlantic subtropical gyre. Science 329, 1185–1188.

Lenz, R., Enders, K., Stedmon, C.A., Mackenzie, D.M., Nielsen, T.G., 2015. A critical assessment of visual identification of marine microplastic using Raman spectroscopy for analysis improvement. Mar. Pollut. Bull. 100, 82–91.

Li, J., Liu, H., Chen, J.P., 2018. Microplastics in freshwater systems: a review on occurrence, environmental effects, and methods for microplastics detection. Water Res. 137, 362–374.

Ling, S.D., Sinclair, M., Levi, C.J., Reeves, S.E., Edgar, G.J., 2017. Ubiquity of microplastics in coastal seafloor sediments. Mar. Pollut. Bull. 121, 104–110.

Lots, F.A., Behrens, P., Vijver, M.G., Horton, A.A., Bosker, T., 2017. A large-scale investigation of microplastic contamination: abundance and characteristics of microplastics in European beach sediment. Mar. Pollut. Bull. 123, 219–226.

Lusher, A.L., Tirelli, V., O'Connor, I., Officer, R., 2015. Microplastics in Arctic polar waters: the first reported values of particles in surface and sub-surface samples. Sci. Rep. 5, 14947.

Mato, Y., Isobe, T., Takada, H., Kanehiro, H., Ohtake, C., Kaminuma, T., 2001. Plastic resin pellets as a transport medium for toxic chemicals in the marine environment. Environ. Sci. Technol. 35, 318–324.

Mauro, R.D., Kupchik, M.J., Benfield, M.C., 2017. Abundant plankton-sized microplastic particles in shelf waters of the northern Gulf of Mexico. Environ. Pollut. 230, 798–809.

Moore, C.J., Moore, S.L., Leecaster, M.K., Weisberg, S.B., 2001. A comparison of plastic and plankton in the north Pacific central gyre. Mar. Pollut. Bull. 42, 1297–1300.

Morét-Ferguson, S., Law, K.L., Proskurowski, G., Murphy, E.K., Peacock, E.E., Reddy, C.M., 2010. The size, mass, and composition of plastic debris in the western North Atlantic Ocean. Mar. Pollut. Bull. 60, 1873–1878.

Murray, F., Cowie, P.R., 2011. Plastic contamination in the decapod crustacean *Nephrops norvegicus* (Linnaeus, 1758). Mar. Pollut. Bull. 62, 1207–1217.

Nauendorf, A., Krause, S., Bigalke, N.K., Gorb, E.V., Gorb, S.N., Haeckel, M., et al., 2016. Microbial colonization and degradation of polyethylene and biodegradable plastic bags in temperate fine-grained organic-rich marine sediments. Mar. Pollut. Bull. 103, 168–178.

NOAA, 2015. Laboratory Methods for the Analysis of Microplastics in the Marine Environment: Recommendations for Quantifying Synthetic Particles in Waters and Sediments. Available from: https://marinedebris.noaa.gov/sites/default/files/publications-files/noaa_microplastics_methods_manual.pdf.

NOAA, 2016. What Are Microplastics? National Ocean Service Available at: https://oceanservice.noaa.gov/facts/microplastics.html

Ogata, Y., Takada, H., Mizukawa, K., Hirai, H., Iwasa, S., Endo, S., et al., 2009. International Pellet Watch: global monitoring of persistent organic pollutants (POPs) in coastal waters. 1. Initial phase data on PCBs, DDTs, and HCHs. Mar. Pollut. Bull. 58, 1437–1446.

Piñon-Colin, T.d.J., Rodriguez-Jimenez, R., Pastrana-Corral, M.A., Rogel-Hernandez, E., Wakida, F.T., 2018. Microplastics on sandy beaches of the Baja California Peninsula, Mexico. Mar. Pollut. Bull. 131, 63–71.

PlasticsEurope, 2018. Plastics - The Facts. , p. 2017. http://www.plasticseurope.org/application/files/5715/1717/4180/Plastics_the_facts_2017_FINAL_for_website_one_page.pdf.

Ribeiro-Claro, P., Nolasco, M.M., Araújo, C., 2016. Chapter 5: characterization and analysis of microplastics. In: Rocha-Santos, T.A.P., Duarte, A.C. (Eds.), Comprehensive Analytical Chemistry. 75. Elsevier, Netherlands, pp. 136–137.

Rochman, C.M., Hentschel, B.T., Teh, S.J., 2014. Long-term sorption of metals is similar among plastic types: implications for plastic debris in aquatic environments. PLoS One 9, e85433.

Rodríguez-Seijo, A., Pereira, R., 2016. Chapter 3: morphological and physical characterization of microplastics. In: Rocha-Santos, T.A.P., Duarte, A.C. (Eds.), Comprehensive Analytical Chemistry. 75. Elsevier, Netherlands, pp. 49–65.

Ryan, P.G., Moore, C.J., van Franeker, J.A., Moloney, C.L., 2009. Monitoring the abundance of plastic debris in the marine environment. Philos. Trans. R. Soc. Lond. B Biol. Sci. 364, 1999–2012.

Song, Y.K., Hong, S.H., Mi, J., Kang, J.H., Kwon, O.Y., Han, G.M., et al., 2014. Large accumulation of micro-sized synthetic polymer particles in the sea surface microlayer. Environ. Sci. Technol. 48, 9014–9021.

Stolte, A., Forster, S., Gerdts, G., Schubert, H., 2015. Microplastic concentrations in beach sediments along the German Baltic coast. Mar. Pollut. Bull. 99, 216–229.

Teuten, E.L., Rowland, S.J., Galloway, T.S., Thompson, R.C., 2007. Potential for plastics to transport hydrophobic contaminants. Environ. Sci. Technol. 41, 7759–7764.

Thompson, R.C., Olsen, Y., Mitchell, R.P., Davis, A., Rowland, S.J., John, A.W., et al., 2004. Lost at sea: where is all the plastic? Science 304, 838.

Vasile, C., Dekker, M., 2000. Handbook of Polyolefins. New York. 2nd ed. (rev. and expanded).

Verran, J., Boyd, R.D., 2001. The relationship between substratum surface roughness and microbiological and organic soiling: a review. Biofouling 17, 59–71.

Vethaak, A.D., Leslie, H.A., 2016. Plastic debris is a human health issue. Environ. Sci. Technol. 50, 6825–6826.

Von Moos, N., Burkhardt-Holm, P., Köhler, A., 2012. Uptake and effects of microplastics on cells and tissue of the blue mussel *Mytilus edulis* L. after an experimental exposure. Environ. Sci. Technol. 46, 11327–11335.

Waller, C.L., Griffiths, H.J., Waluda, C.M., Thorpe, S.E., Loaiza, I., Moreno, B., et al., 2017. Microplastics in the Antarctic marine system: an emerging area of research. Sci. Total Environ. 598, 220–227.

Watts, A.J.R., Urbina, M.A., Corr, S., Lewis, C., Galloway, T.S., 2015. Ingestion of plastic microfibers by the crab *Carcinus maenas* and its effect on food consumption and energy balance. Environ. Sci. Technol. 49, 14597–14604.

Wegner, A., Besseling, E., Foekema, E.M., Kamermans, P., Koelmans, A.A., 2012. Effects of nanopolystyrene on the feeding behavior of the blue mussel (*Mytilus edulis* L.). Environ. Toxicol. Chem. 31, 2490–2497.

Wessel, C.C., Lockridge, G.R., Battiste, D., Cebrian, J., 2016. Abundance and characteristics of microplastics in beach sediments: insights into microplastic accumulation in northern Gulf of Mexico estuaries. Mar. Pollut. Bull. 109, 178–183.

Wright, S.L., Kelly, F.J., 2017. Plastic and human health: a micro issue? Environ. Sci. Technol. 51, 6634–6647.

Wright, S.L., Rowe, D., Thompson, R.C., Galloway, T.S., 2013a. Microplastic ingestion decreases energy reserves in marine worms. Curr. Biol. 23, 1031–1033.

Wright, S.L., Thompson, R.C., Galloway, T.S., 2013b. The physical impacts of microplastics on marine organisms: a review. Environ. Pollut. 178, 483–492.

Yamashita, R., Tanimura, A., 2007. Floating plastic in the Kuroshio Current area, western North Pacific Ocean. Mar. Pollut. Bull. 54, 485–488.

Yuan, Y., Liao, G., Yang, C., Liu, Z., Chen, H., Wang, Z.G., 2014. Summer Kuroshio Intrusion through the Luzon Strait confirmed from observations and a diagnostic model in summer 2009. Prog. Oceanogr. 121, 44–59.

Zhang, H., 2017. Transport of microplastics in coastal seas. Estuar. Coast. Shelf Sci. 119, 74–86.

Zhang, W., Zhang, S., Wang, J., Wang, Y., Mu, J., Wang, P., et al., 2017. Microplastic pollution in the surface waters of the Bohai Sea, China. Environ. Pollut. 231, 541–548.